Dalton Transactions

Accepted Manuscript

ROYAL SOCIETY OF CHEMISTRY

www.rsc.org/dalton

Cite this: DOI: 10.1039/c0xx00000x

www.rsc.org/xxxxxx

ARTICLE TYPE

Assembling CdS mesoporous nanosheets into 3D hierarchitectures for effectively photocatalytic performance

Chengzhen Wei,[a] Cheng Cheng,[a] Junhong Zhao,[a] Shasha Zheng,[a] Mingming Hao[a] and Huan Pang*[a, b]

Received (in XXX, XXX) Xth XXXXXXXXX 20XX, Accepted Xth XXXXXXXXX 20XX
DOI: 10.1039/b000000x

3D hierarchical CdS assembled with mesoporous nanosheets are prepared via a facile hydrothermal method in the presence of soulcarboxymthyi chitosan. By investigation of various reaction parameters, it is demonstrated that the reaction temperature and the amount of ammonia, thiourea and $Cd(NO_3)_2$ play important roles in the formation of 3D hierarchical CdS. The optical property of 3D hierarchical CdS is investigated by ultraviolet-visible (UV-vis) spectroscopy. The photocatalytic activity experiment reveals that the as-synthesized 3D hierarchical CdS exhibits an excellent photocatalytic performance for the degradation of methyl orange (MO) aqueous solution under the visible-light illumination, suggesting that the 3D hierarchical CdS nanomaterial might be used as a promising candidate for the treatment organic pollutants in the waste water.

1. Introduction

During the past decades, the controlled synthesis of inorganic macro/nanostructured materials with desired morphology and dimensionality has attracted considerable interest for their distinctive properties.[1-5] In particular, 3D hierarchical structures with porous materials, which are able to interact with liquids and gases not only at the surface, but also in the inner part of the materials, have been attracting considerable attention for their broad applications in catalytic, sensors, energy storage, environment protection and biomedical fields. Therefore, the design and fabrication of 3D hierarchical structures with porous materials represents a hot topic in the material fields.[6-17] So far, several approaches have been reported for the fabrication of 3D hierarchical structures materials. Among them, hydrothermal treatment is one of the simplest routes owing to its easily tunable synthesis condition.

As an important II-VI semiconductor, CdS with a direct band gap of 2.5 eV has been extensively studied because of its promising application in catalysis, optical materials and photonics. [18-21] Recently, some 3D hierarchical structures CdS materials such as dendritic, urchin-like nanoflowers, flower/sphere networks and hyperbranched, [22-25] have been successfully fabricated to improve their physical and chemical properties. However, the development of convenient and feasible approach for synthesis of 3D hierarchical CdS is expected to be further development. Biomolecule assisted-synthesis has been proven to be a new focus and promising routes in the preparation of metal chalcogenides 3D hierarchical structures because of its convenience, environmentally friendly and strong function in morphology control. For example, PbS, In_2S_3, Ni_3S_2, and Bi_2S_3 3D hierarchical structures have been fabricated through the biomolecule assisted-synthesis route. [26-29] More importantly, CdS with various morphologies recently have also been prepared via the biomolecule assisted-synthesis route. [30, 31] Soulcarboxymthyi chitosan is a kind of representative polyanion green biomolecular and has been widely used in biomedical fields, [32] which contains a large number of carboxymethyl groups and has ability to coordinate with Cd^{2+}. Therefore, these reasons inspired the use of soulcarboxymthyi chitosan in the preparation of nanomaterials.

Herein, we firstly present a simple hydrothermal approach to prepare 3D hierarchical mesoporous CdS in the presence of soulcarboxymthyi chitosan. Moreover, the effect of the experimental parameters on the morphology of 3D hierarchical structures CdS was further studied. More importantly, the photocatalytic activity of as-prepared 3D hierarchical structures CdS was also evaluated by the degradation of MO aqueous solution under visible-light illumination.

2. Experimental Section

2.1 The synthesis of 3D hierarchical CdS

In a typical synthesis, 0.5 mmol $Cd(NO_3)_2{\cdot}5H_2O$ (analytically pure) was dissolved in 7.0 mL of deionized water with magnetic stirring, then 3.0 mL of ammonia solution (25%, analytically pure) and 3.0 mmol thiourea (analytically pure) were added, followed by the addition of a solution of 10.0 mL of 11.2 g L^{-1} soulcarboxymthyi chitosan aqueous solution. After stirring for 5 min, the resulting solution was transferred into a 50 mL autoclave. The autoclave was sealed, heated at 80 ºC for 6 h and cooled down to room temperature naturally. The precipitate was collected by centrifugation under 3000 rpm min^{-1} for 10 minutes and washed with distilled water and ethanol several times, then dried at 50 ºC for 12 h.

2.2 Characterizations

The phase of these obtained samples was characterized by X-ray diffraction (XRD) with a Shimadzu XRD-6000 powder X-ray diffractometer with Cu K_α radiation (λ=1.5418 Å). The morphology of the samples was taken by a Hitachi S-4800 field-emission scanning electron microscope (FE-SEM) at an acceleration voltage of 10.0 KV. Transmission electron

microscopy (TEM), high-resolution TEM (HRTEM) images and the corresponding selected area electron diffraction (SAED) were obtained on the JEOL JEM-2100 instrument microscopy at an acceleration voltage of 200 KV. The UV-vis diffusion reflectance spectrum (DRS) of the samples was studied with a UV-vis spectrophotometer (UV-3600, Shimadzu, Japan) and $BaSO_4$ was used as reference. The surface area, pore size, and pore size distribution of the products were determined by BrunauerEmmett-Teller (BET) nitrogen adsorption-desorption and Barett-Joyner-Halenda (BJH) methods (Micromeritics, ASAP2020).

2.3 Photocatalytic experiments

The photocatalytic activities of the as-synthesized samples for photocatalytic decolorization of MO aqueous solution were performed as follows: A 300 W xenon lamp was used as the visible light source with a cutoff filter to cut off the light below 420 nm. Before being irradiated, the suspensions were continuously magnetically stirred in the dark for 30 min to establish an adsorption/desorption equilibrium between CdS powder and the dye. Then, the photocatalytic reaction was initiated. At given time intervals, a series of aqueous solutions were taken from the reaction cell and separated through centrifugation (10000 rpm/min) for absorbance measurements, which were recorded with a Hitachi U-3900 spectrophotometer.

3. Results and Discussion

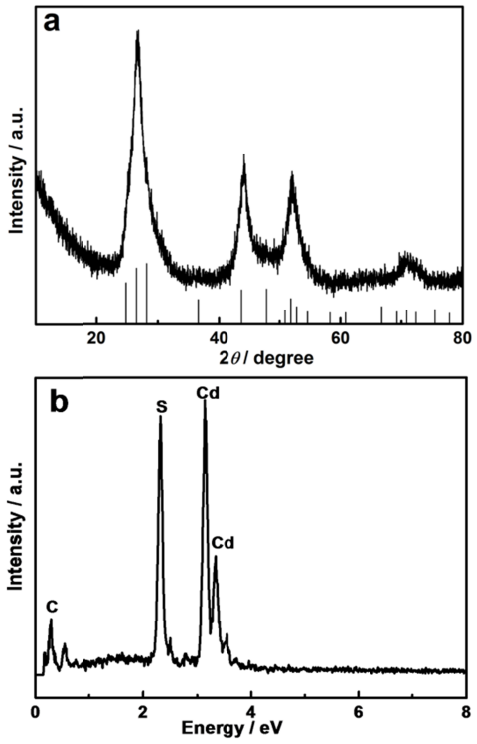

Fig. 1 (a) XRD pattern, and (b) EDS spectrum of the as-synthesized samples.

The phase composition and purity of the as-prepared products were characterized by X-ray diffraction (XRD). Fig. 1a shows a typical XRD pattern of the as-prepared sample. All of the diffraction peaks can be perfectly indexed to that of hexagonal wurtzite CdS (JCPDS No. 41-1049). No characteristic peaks corresponding to other impurities were found in this pattern, which indicated the high purity of the product. The chemical composition of the as-prepared sample was also determined by energy dispersive X-ray spectroscopy (EDS). As shown in Fig. 1b, the EDS spectrum displays strong peaks of C, Cd and S. The peak of C is due to the carbon on the conductive adhesive tape used to hold the sample for SEM observations. Quantitative analysis confirmed that the atom ratio of Cd to S is about 1:1, indicating a normal composition of CdS. All these results confirmed that the as-obtained sample is the pure CdS phase.

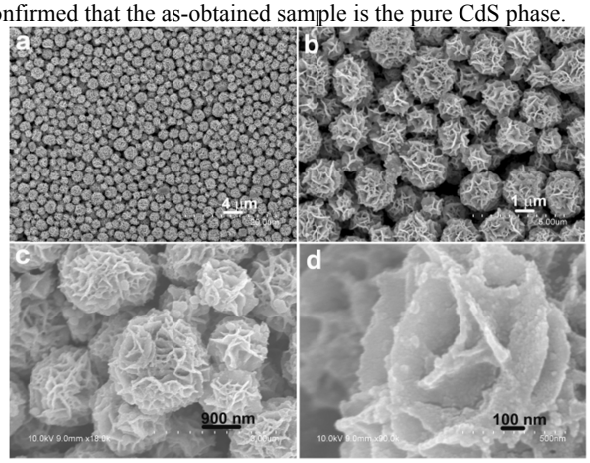

Fig. 2 SEM images of the as-synthesized 3D hierarchical CdS.

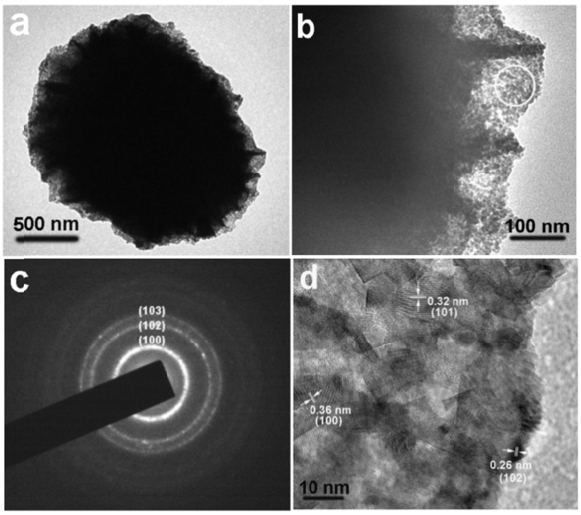

Fig. 3 TEM images of (a, b) 3D hierarchical CdS; (c, d) the SAED pattern, and HRTEM image from the area marked with the white cycle in inset of b.

The morphologies and structures of the as-prepared CdS sample were examined by FE-SEM and TEM. As shown in Fig. 2, a panoramic SEM image (Fig. 2a) shows that the sample consists of 3D hierarchical structures with average diameter of 2 μm. The magnified SEM images (Fig. 2b, c) reveal that the 3D hierarchical CdS is well assembled by many interleaving nanosheets. After the further magnification in Fig. 2d, it is found that the thickness of the nanosheet is about 20 nm, and the nanosheet is constructed by many small nanoparticles.

Fig. 3a displays a TEM image of a representative 3D

hierarchical CdS, and Fig. 3b shows the corresponding high-magnification image. It is obviously found that the nanosheet has a unique porous structure composed of many nanoparticles. Fig. 3c shows the corresponding SAED pattern taken from the nanosheet of 3D hierarchical CdS. The diffraction rings suggest the nanosheet is polycrystalline in nature. The HRTEM image (Fig. 3d) obtained from the area marked with white pane shown in Fig. 3b also confirms that the nanosheet is polycrystalline, the fringe spacings 0.26 nm, 0.32 nm and 0.36 nm are consistent with the interplanar of (102), (101) and (100) lattice planes, respectively.

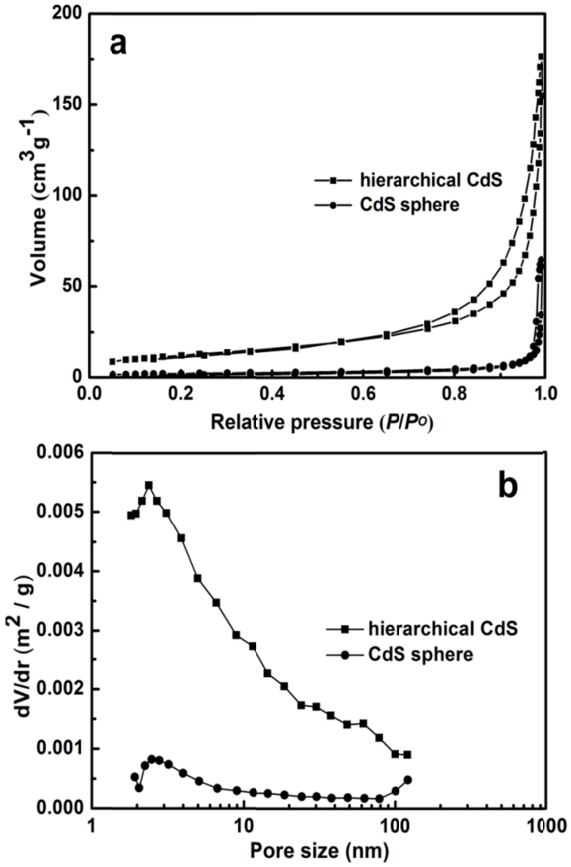

Fig. 4 (a) N_2 adsorption-desorption isotherms of as-prepared CdS samples; (b) Corresponding pore size distribution curves of as-prepared CdS samples .

To gain further insight into the porous structure and pore size distribution of samples, Brunauer-Emmett-Teller (BET) measurements were performed to examine their specific structural properties. As shown in Fig. 4a, the BET surface area of 3D hierarchical CdS (42.26 $m^2 g^{-1}$) is much larger than that of solid CdS sphere (7.08 $m^2 g^{-1}$). The Barrett-Joyner-Halenda (BJH) pore size distribution curves (Fig. 4b) shows that the pore size for 3D hierarchical CdS is in the range of the mesopores (2-5 nm), indicating the mesopores possibly formed by porous stacking of component nanoparticles, while the solid CdS sphere has few pores.

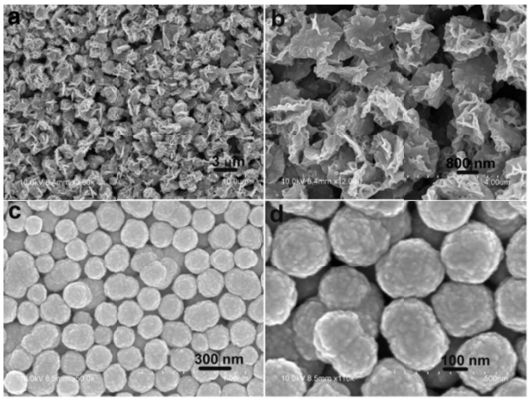

Fig. 5 SEM images of the sample obtained at different amounts of ammonia: (a, b) 1.0 mL, (c, d) 4.0 mL.

In this work, the addition of ammonia and soulcarboxymthyi chitosan is crucial factor to the formation of such 3D hierarchical CdS. Without adding ammonia into the reaction system, unfortunately, we could not obtain sample. This result is reasonable, thiourea could not easily be decomposed under low temperature. When ammonia was introduced into the reaction solution, the basic of the solution could be increased. Thiourea could be decomposed under the basic condition at the same reaction temperature. By decreasing the volume of ammonia to 1.0 mL, while other conditions were kept constant, disklike structures could be obtained (Fig. 5a, b). When the volume of ammonia was increased to 4.0 mL, CdS nanospheres are observed (Fig. 5c, d). This phenomenon can be explained that the pH value of the reaction solution was increased remarkably with adding 4.0 mL ammonia into the solution. Thiourea could be decomposed fast under strong basic condition. Then CdS nanoparticles formed and soon assembled into nanosphere with the assistance of soulcarboxymthyi chitosan. Interestingly, by replacing ammonia with NaOH aqueous solution, we obtain CdS nanoparticles instead of novel 3D hierarchical CdS in the reaction system (Fig. S1 in the electronic supplementary information). As is known, the basic of NaOH is much stronger than ammonia, the change of the reaction system pH can affect the growth of CdS crystal. Therefore, in our reaction system, a certain volume of ammonia is suitable for the formation of 3D hierarchical CdS structures.

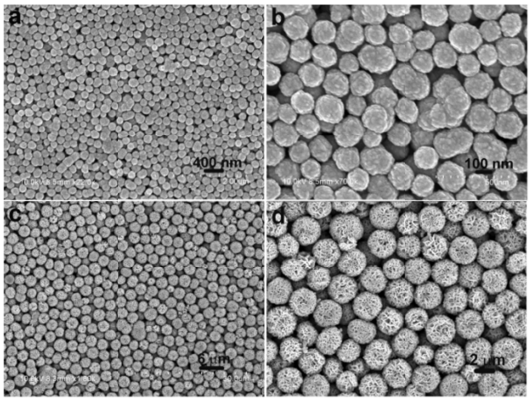

Fig. 6 SEM images of the sample obtained at different amounts of $Cd(NO_3)_2$: (a, b) 0.25 mmol, (c, d) 1.0 mmol.

The controlled experiments have also shown that the biomolecule soulcarboxymthyi chitosan is crucial to the formation of well-defined CdS 3D hierarchical structures. When there was no soulcarboxymthyi chitosan being used, irregular CdS assembled with nanosheet could be obtained (Fig. S2). This result directly confirmed that the soulcarboxymthyi chitosan could promote the delicate assembly. As is known, the soulcarboxymthyi chitosan molecules contain a large number of carboxymethyl groups, such that the carboxymethyl groups can coordinate with Cd^{2+}.[33] The soulcarboxymthyi chitosan molecules play important roles: a) preventing the aggregation of CdS nanoparticles in the initial nucleation stage via coordination with Cd^{2+}, and b) kinetically controlling the growth rates of CdS crystals, which induce the formation of perfectly 3D hierarchical CdS.

Furthermore, it was also found that the morphologies of 3D hierarchical CdS structures were sensitive to the amount of reagents and the reaction temperatures. For example, by decreasing the amount of $Cd(NO_3)_2$ from 0.50 mmol to 0.25 mmol while keeping other experimental conditions unchanged, only CdS nanospheres are (were)obtained (Fig. 6a, b). However, when the amount of $Cd(NO_3)_2$ is(was) increased to 1.0 mmol, no significant morphology change is found (Fig. 6c, d).

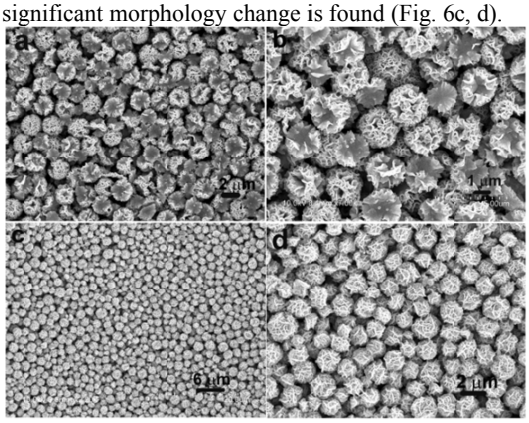

Fig. 7 SEM images of the sample obtained at different amounts of thiourea: (a, b) 1.0 mmol, (c, d) 6.0 mmol.

As shown in Fig. 7a, b, when the amount of thiourea was 1.0 mmol, disklike morphology and flowerlike structures CdS could be obtained. When increasing the amount of thiourea to 6.0 mmol, the 3D hierarchical CdS assembled with nanosheets was observed (Fig. 7c, d). The successful fabrication of 3D hierarchical CdS structures assembled with nanosheets revealed that thiourea functions were not only as the S source but also as the shape controlling agent in the reaction process.

Moreover, when the reaction temperature was decreased to 60 ºC, the perfect 3D hierarchical CdS structures were prepared (Fig. 8a, b). Increasing the reaction temperature to 120 ºC, we could only acquire CdS nanospheres (Fig. 8c, d). It might be related to the reaction rate increased at high temperature. Furthermore, the reaction rate could alter the growth process of CdS crystals in the present reaction system, leading to the formation of the CdS nanospheres at 120 °C. Based on the above discussion, it was found that the high reaction temperature was not suitable for the formation of 3D hierarchical CdS in our reaction system.

Interestingly, no 3D hierarchical CdS structures were obtained by replacing thiourea with thioacetamide (Fig. S3). Comparing with thiourea, the hydrolysis rate of thioacetamide to release S^{2-} is more quickly, CdS nanoparticles soon formed and have not enough time to form 3D hierarchical structures. It indicated that the formation of the flowerlike structures might be dependent on the special properties of thiourea. When $CdCl_2$ or $Cd(AC)_2$ was used as the cadmium source instead of $Cd(NO_3)_2$, the morphologies of the products were not changed (Fig. 9), comparing with the typical synthesis condition.

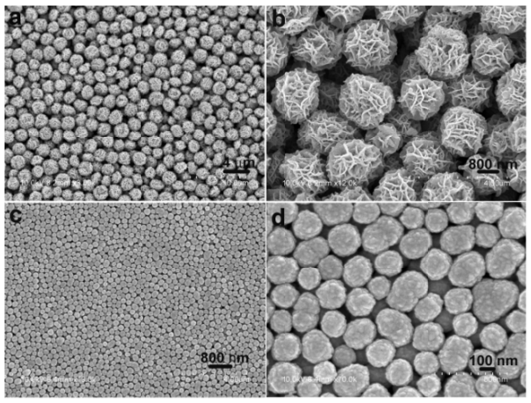

Fig. 8 SEM images of the sample obtained at different reaction temperature: (a, b) 60 ºC, (c, d) 120 ºC.

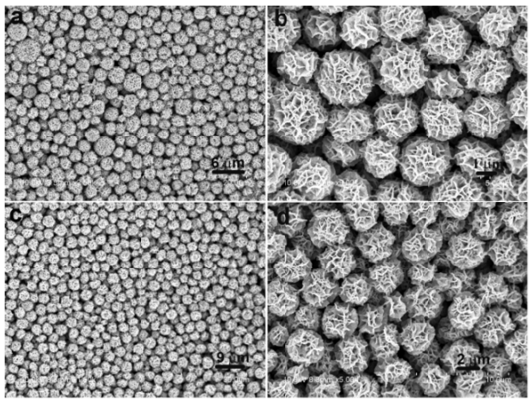

Fig. 9 SEM images of the CdS prepared from different cadmium source: (a,b) $Cd(Ac)_2$, (c,d) $CdCl_2$.

The UV-visible diffuse reflectance was employed for studying the optical properties of the 3D hierarchical and solid sphere CdS. As shown in Fig. 10A, it can be found that both of them have a strong absorption in the range of visible-light region because of the intrinsic band gap absorption of CdS. The 3D hierarchical and solid CdS spheres have an absorption edge at about 567 nm and 563 nm, respectively. The absorption edge for the 3D hierarchical CdS at visible-light region showed a red-shift, comparing with the solid CdS spheres. It demonstrates that the band gap of 3D hierarchical CdS was smaller than that of solid CdS spheres. As a crystalline semiconductor, the optical absorption near the band edge follows the formula $(Ah\nu)^n = B(h\nu - E_g)$, where A, $h\nu$, E_g and B are the absorption coefficient, photon energy, band gap, and a constant, respectively. Among them, "n" is an index determined by the nature of electron transition in a semiconductor, which is either 2 for direct inter-band transition or 1/2 for indirect inter-band transition.[34, 35] In this manuscript, for

CdS, it is a case of semiconductor of direct band gap, and the value of n is 2 for the direct transition. Fig. 10B presents the $(Ah\nu)^2$ versus photon energy ($h\nu$) curve for CdS samples. The bang gap energies (E_g values) of the CdS samples can be estimated by extrapolating the straight portion of $(Ah\nu)^2$ - $h\nu$ plot to the point A = 0. Therefore, the band gaps calculated by this approach are about 2.18 eV and 2.20 eV for the 3D hierarchical CdS and solid CdS spheres, respectively. The band gap of 3D hierarchical CdS is narrower than the value of solid CdS spheres. The possible reason is its specific structure. In general, the interaction among the lattice binding, the free electrons and holes can lead the band gap to a narrow one. [36] The experimental results suggested that the 3D hierarchical CdS have great potential as photocatalysts to decompose organic pollutants under visible-light irradiation.

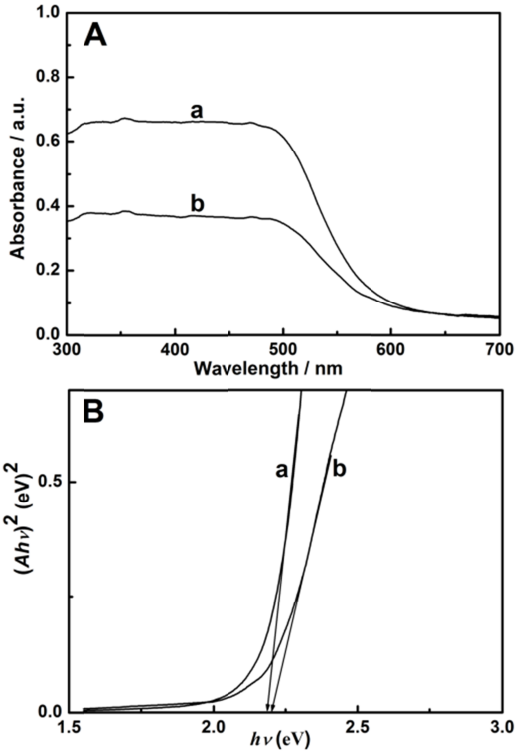

Fig. 10 (A) UV-vis diffuse reflectance spectra of the as-prepared CdS samples: (a) 3D hierarchical CdS; (b) solid CdS sphere, (B) Plots of the $(ah\nu)^2$ versus $h\nu$ of the CdS samples: (a) 3D hierarchical CdS; (b) solid CdS sphere.

The photocatalytic performance of as-synthesized 3D hierarchical CdS was studied by photocatalytic decolorization of MO aqueous solution. Fig. 11a shows the absorption spectra of MO aqueous solution in the presence of 3D hierarchical CdS under visible-light for various irradiation times. With the increasing of irradiation time, the intensity of the characteristic absorption peak drops obviously. The concentration curve of residual MO as a function of irradiation time is shown in Fig. 11b. After being irradiated with visible light for 100 min in the presence of 3D hierarchical CdS, the MO was almost completely degraded. In contrast, about 89% of the MO was degraded after being irradiated 100 min for the solid CdS spheres. The 3D hierarchical CdS showed the best photocatalytic performace for MO degradation, which might be related to the special structure. Specifically, the higher specific surface area could increase the contact area between the CdS and MO aqueous solution. It has been reported that large specific surface area not only helped increase the photocatalytic reaction sites but also promoted the efficiency of the electron hole separation. In addition, 3D hierarchical CdS with pores could benefit the transfer of the light generated charging to the surface to react with the organic molecules, which allowed the rapid diffusion of the reactants and products during the reaction. [37, 38] Without adding catalyst, it was found that the MO was nearly not degraded under visible-light irradiation condition. These results suggest that 3D hierarchical CdS is an effective catalyst for decolorization of methyl-orange solution, and its photocatalytic activity is superior to that of CdS hollow spheres and flower like CdS.[6, 39] More importantly, the photocatalytic activity of as-prepared 3D hierarchical CdS is also superior to that of other photocatalytic materials, such as TiO_2, ZnO, SnO_2 and Cu/C materials.[40-42] Based on the above discussion, it demonstrate that the 3D hierarchical CdS have a good photocatalytic activity under the visible-light region and might be used as a promising photocatalyst for treating organic pollutants in the waste water.

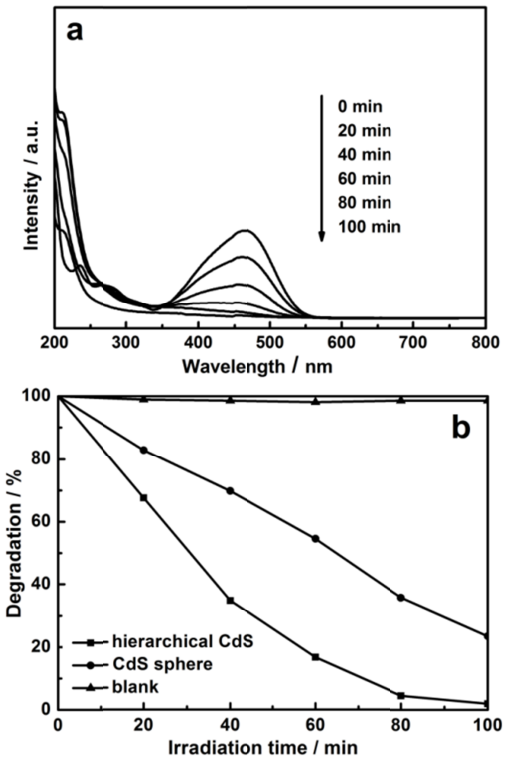

Fig. 11 (a) Absorption spectrum of a solution of MO in the presence of 3D hierarchical CdS under visible light irradiation, (b) The photodegration efficiency of MO as a function of irradiation time.

4. Conclusions

In summary, a facile and economical hydrothermal synthetic method was developed to fabricate 3D hierarchical CdS with mesoporous nanosheets. The investigation shows that the amount

of ammonia, thiourea and $Cd(NO_3)_2$, and the reaction temperature play important roles in the formation of 3D hierarchical CdS. The as-prepared 3D hierarchical CdS exhibited a higher photocatalytic performance for the photocatalytic degradation of MO due to its specific structures. Because of the facile and economical synthesis and controlled morphology, the prepared 3D hierarchical CdS may be used as potential applications in catalysis and other fields.

Acknowledgements

This work is supported by the National Natural Science Foundation of China (NSFC 21201010, 21003001 and 21071006), Science and Technology Foundation of Henan Province (122102210253), China Postdoctoral Science Foundation (2012M521115).

Notes and references

[a] *College of Chemistry and Chemical Engineering, Anyang Normal University, Anyang, 455000 Henan, P. R. China.*
E-mail: huanpangchem@hotmail.com
[b] *State Key Laboratory of Coordination Chemistry, Nanjing University, Nanjing, 210093 Jiangsu, P. R. China*

1 D. Kim, N. Lee, M. Park, B. H. Kim, K. An and T. Hyeon, *J. A. Chem. Soc*., 2009, **131**, 454.
2 M. Han, Y. R. Li, H. Y. Niu, L. L. Liu, K. J. Chen, J. C. Bao, Z. H. Dai and J. M. Zhu, *Chem.- Eur. J*., 2011, **17**, 3739.
3 G. X. Zhu, H. Xu, Y. Y. Xiao, Y. J. Liu, A. H. Yuan and X. P. Shen, *ACS Appl. Mater. Interfaces*, 2012, **4**, 744.
4 W. Z. Li, L. Kuai, L. Chen and B. Y. Geng, *Sci. Rep*. 2013, **3**, 2377; DOI: 10. 1038/srep02377.
5 L, Z. Zhou, L. Kuai, W. Z. Li, and B. Y. Geng, *ACS Appl. Mater. Interfaces*, 2012, **4**, 6463.
6 C. Z. Wei, W. Z. Zang, J. Z. Yin, Q. Y. Lu, Q. Chen, R. M. Liu and F. Gao, *ChemPhysChem*, 2013, **14**, 591.
7 H. Pang, F. Gao, Q. Chen, R. M. Liu and Q. Y. Lu, *Dalton Trans*., 2012, **41**, 5862.
8 H. Pang, Q. Y. Lu, J. J. Wang, Y. C. Li and F. Gao, *Chem. Commun*., 2010, **46**, 2010.
9 H. Pang, Y. Y. Liu, Y. H. Ma, G. C. Li, Y. N. Ai, J. Chen, J. S. Zhang and H. H. Zheng, *Nanoscale*, 2013, **5**, 503.
10 H. B. Wu, H. Pang and X. W. Lou, *Energy Environ. Sci.*, 2013, **6**, 3619.
11 Y. Jiang, H. F. Gong, D. Volkmer, L. B. Gower and H. Cölfen, *Adv. Mater*., 2011, **23**, 3548.
12 Y. Wang, S. K. Li, X. R. Xing, F. Z. Huang, Y. H. Shen, A. J. Xie, X. F. Wang and J. Zhang, *Chem.- Eur. J*., 2011, **17**, 4802.
13 X. H. Liu, J. Zhang, L. W. Wang, T. L. Yang, X. Z. Guo, S. H. Wu and S. R. Wang, *J. Mater. Chem*., 2011, **21**, 349.
14 K. B. Xu, R. J. Zou, W. Y. Li, Y. F. Xue, G. S. Song, Q. Liu, X. J. Liu and J. Q. Hu, *J. Mater. Chem. A*., 2013, **1**, 9107.
15 X. H. Zhang, Y. N. Li and C. B. Cao, *J. Mater. Chem*., 2012, **22**, 13918.
16 S. W. Cao and Y. J. Zhu, *J. Phys. Chem. C*, 2008, **112**, 12149.
17 B. Y. Geng, B. Tao, X. L. Li and W. J. Wei, *Nanoscale*, 2012, **4**, 1671.
18 Y. Y. Huang, F. Q. Sun, H. J. Wang, Y. He, L. S. Li, Z. X. Huang, Q. S. Wu and J. C. Yu. *J. Mater. Chem*., 2009, **19**, 6901.
19 J. G. Yu, J. Zhang and M. Jaroniec, *Green Chem.*, 2010, **12**, 1611.
20 Y. C. Zhang, G. Y. Wang and X. Y. Hu, *J. Alloys. Compd*., 2007, **437**, 47.
21 B. Liu, R. Chen, X. L. Xu, D. H. Li, Y. Y. Zhao, Z. X. Shen, Q. H. Xiong and H. D. Sun, *J. Phys. Chem. C*, 2011, **115**, 12826.
22 D. J. Wang, D. S. Li, L. Guo, F. Fu, Z. P. Zhang and Q. T. Wei, *J. Phys. Chem. C*, 2009, **113**, 5984.
23 W. T. Yao, S. H. Yu, S. J. Liu, J. P. Chen, X. M. Liu and F. Q. Li, *J. Phys. Chem. B*, 2006, **110**, 11704.
24 S. L. Xiong, X. G. Zhang and Y. T. Qian, *Cryst. Growth Des*, 2009, **9**, 5259.
25 M. H. Chen, Y. N. Kim, C. C. Li and S. O. Cho, *Cryst. Growth Des*, 2008, **8**, 629.
26 X. F. Shen, and X. P. Yan, *Angew. Chem., Int. Ed*. 2007, **46**, 7659.
27 L. Y. Chen, Z. D. Zhang and W. Z. Wang, *J. Phys. Chem. C*, 2008, **112**, 4117.
28 B. Zhang, X. C. Ye, W. Dai, W. Y. Hou and Y. Xie, *Chem.- Eur. J*., 2006, **12**, 2337.
29 Q. Y. Lu, F. Gao and S. Komarneni, *J. Am. Chem. Soc*., 2004, **126**, 54.
30 F. Gao, Q. Y. Lu, X. K. Meng and S. Komarneni, *J. Phys. Chem. C*, 2008, **112**, 13359.
31 S. L. Xiong, B. J. Xi, C. M. Wang, G. F. Zou, L. F. Fei, W. Z. Wang and Y. T. Qian, *Chem.- Eur. J*., 2007, **13**, 3076.
32 N. Nishi, H. Ohnuma, S. I. Nishimura, O. Somorin and S. Tokura. *Polym J*, 1982, **14**, 919.
33 J. Z. Yin, F. Gao, J. J. Wang and Q. Y. Lu, *Chem. Commun*., 2011, **47**, 4141.
34 L. P. Zhu, G. H. Liu, N. C. Bing, L. L. Wang, Y. Yang and H. Y. Xie, *CrystEngComm*., 2010, **12**, 3791.
35 L. Chen, S. F. Yin, R. Huang, Q. Zhang, S. L. Luo and C. T. Au, *CrystEngComm*., 2012, **14**,4217.
36 T. Y. Zhao, J. T. Zai, M. Xu, Q. Zou, Y. Z. Su, K. X. Wang and X. F. Qian, *CrystEngComm*., 2011, **13**, 4010.
37 D. Li and Y. F. Zhu, *CrystEngComm*., 2012, **14**, 1128.
38 L. Z. Zhang and J. C. Yu, *Chem. Commun*., 2003, 2078.
39 Y. C. Zhang, Z. N. Du, K. W. Li and M. Zhang, *Sep. Purif. Technol*, 2011, **81**, 101.
40 Y. R. Zhang, J. Wan and Y. Q. Ke, *J. Hazard. Mater*. 2010, **177**, 750.
41 W. W. Wang, Y. J. Zhu and L. X. Yang, *Adv. Funct. Mater*. 2007, **17**, 59.
42 F. Gao, H. Pang, S. P. Xu and Q. Y. Lu, *Chem. Commun*., 2009, 3571.

Table of Contents

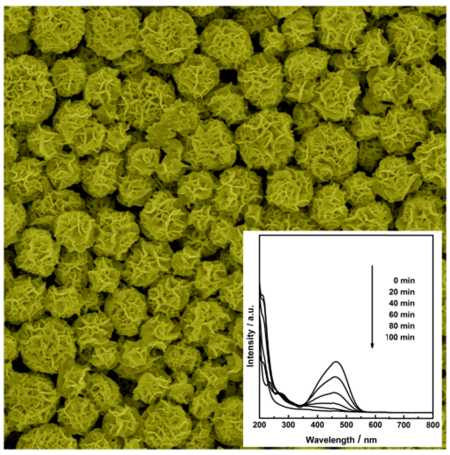

3D hierarchical CdS with mesoporous nanosheets are successfully synthesized via a simple hydrothermal approach, due to its specific 3D hierarchical structures, which exhibits good photocatalytic activity for the degradation of MO.